Informational properties of surface acoustic waves generated by laser-material interactions during laser precision machining
Bordatchev, Evgueni V.; Nikumb, Suwas K.

National Research Council Canada   Conseil national de recherches Canada

Canada

Informational Properties of Surface Acoustic Waves
Generated by Laser-Material Interactions During Laser Precision Machining

Evgueni V. Bordatchev* and Suwas N. Nikumb

Integrated Manufacturing Technologies Institute, National Research Council of Canada

800 Collip Circle, London, Ontario, Canada N6G 4X8

ABSTRACT

Laser precision machining is primarily a CNC-based technology; therefore, the need for on-line process monitoring and control system is very high, mainly because under usual circumstances the operator has to make a host of complex decisions, based on trial-and-error method, to set the process control parameters related to laser, optics, workpiece material, and motion system. However, the crucial element of any control system is the information about the process and system's dynamics. The problem of choosing reliable and at the same time physically observed information on process parameters becomes more complicated in the case of laser precision machining where the laser-material interactions generate a number of emissions with a different physical nature. To capture the informational properties from the measured signals and parameters for the purpose of monitoring and control of the process, a thorough understanding of the entire laser-machining system performance and the laser-material interactions is required. This paper describes a method for the analysis of informational properties of surface acoustic waves to generate the knowledge as an informational basis for future development of on-line monitoring and process control systems. The study involves measurement of the acoustic emission signal from the laser-material interaction zone, the statistical and spectral signatures and pattern recognition analysis to select informational parameters, which could reliably correlate with variations within the incident laser pulse energy.

1. INTRODUCTION

During the last decade, laser precision machining has attracted significant interest from modern industry, which is continuously looking for new technologies and machines to make products smaller, more precise and at lower cost. Generally, "direct-write" laser machining [1-5] is based on standard CNC technology and therefore recent developments are focused on the design and control of the laser machine tools [6-10], optimization of process parameters [11,12], and the process control [13-22]. It is essential to control the process because the operator must make a series of complex decisions, based on trial-and-error method, to optimize process control parameters related to laser, optics, workpiece material, and the motion system. In addition, inherent factors such as power fluctuations, intensity distribution, and thermal effects within the optical components, normally not controlled externally, also influence the machining

---

* Corresponding author. Tel.: 1-519-430-7107; fax: 1-519-430-7064; e-mail: evgueni.bordatchev@nrc.ca

process. Furthermore, the problem of choosing the optimal process parameters becomes more complicated when parts and features dimensions become particularly smaller (less than a few tens of microns), when the thermodynamic processes within the laser-material interaction zone could significantly dominate a change in the part geometry. Therefore, the geometric quality of a machined part is the result of the complex dynamic performance of an entire laser machining system along with the dynamics of motion system, on going random changes in laser beam parameters, and the laser-material interactions.

A fundamental necessity in the development of any process control system is the need for reliable and physically observable information about the on going process. During laser machining, interaction of the laser beam with material generates a variety of emissions, such as photonic, optical, thermionic, sonic/ultrasonic acoustic, emerging out of the processing zone. Numerous experimental and theoretical investigations have been carried out in the literature using a variety of sensing techniques for laser-material interactions [14-30]. Sonic emission, due to resonance that is created when the gas jet impinges on the erosion front, was intensively studied [2, 13-16]. The sonic signal was acquired by a wide-band microphone within a frequency range of up to 30 KHz, and was analyzed to determine the erosion front geometry, hole depth and groove depth. The quality of laser cleaning was analyzed and controlled by using a sonic wave as the feedback signal [17]. Another approach for in-process monitoring for laser cleaning was applied by Lee *et al.* [18,19], where a combination of sonic emission and the spectral signature of polychromatic light from the processing zone was analyzed. Using numerical analysis of the frequency characteristic of the sonic signal generated during laser processing, the relationship between the sound pressure level and the material removal area per pulse was studied by Kurita *et al.* [20,21]. The study of acoustic signals from laser back reflections was presented by Weerasinghe *et al.* [22]. The advantage of Weerasinghe's study is that several different sensors, a pyroelectric detector, piezoelectric acoustic transducer, and photodiode, were used to analyse different physical properties of the laser-material interaction simultaneously. The correlation between various signals was investigated. For process monitoring during laser beam cutting [23] a photodiode with sensitivity from 450 to 1100 nm wavelength was used to monitor the correlation between the average surface roughness and standard deviation of the signal. Observations on temperature gradient were investigated by Haferkamp *et al.* [24] to monitor the cut quality, e.g. dross attachment, surface roughness of the kerf and the width of the kerf.

The brief review presented above is by no means intended to be a thorough state-of-the-art work in the literature. However, the intention is to indicate the problems associated with experimental studies on laser-material interactions. Applications of standard sonic techniques using microphones and contact transducers have demonstrated the feasibility of monitoring the state of laser-material interactions and some parameters of a machined surface. It should be noted that all previous studies deal with continuous machining processes like cutting or grooving using either pulsed or CW lasers. This paper presents analysis of the surface acoustic waves, generated by a single laser pulse, with a wide frequency range of up to 500 KHz. The objective of this work is to lay an informational foundation for understanding of

complex physical processes in the laser-material interaction zone and for the development of intelligent process monitoring and control systems for laser precision machining. The study is based on an experimental investigation of the surface acoustic waves and involves the measurement of the acoustic emission signal from the laser-material interaction zone, the statistical and spectral signature analysis, and pattern recognition analysis to select informational parameters, which are reliably correlated with variations within laser pulse energy.

2. CONCEPT OF LASER PRECISION MACHINING

During the laser machining process, laser pulses are applied according to a prescribed toolpath for material removal [1,2]. Each laser pulse removes a certain quantity of material. The geometry and the volume of material removed depend on the material properties and the laser pulse characteristics. Figure 1 shows the schematics of the laser precision machining, which involves a set of process parameters: E - the pulse energy (J); f - the frequency of laser pulses (Hz); d - the focal spot diameter (mm), assuming that the focal spot is circular for TEM00 mode; and v - the travel speed of the workpiece (mm/s). Each laser pulse vaporizes a certain amount of material and produces a crater in the workpiece material. The crater profile is approximated by a circular paraboloid with a height h (machined depth for one path), diameter d, and volume $V = \pi d^2 h/2$. The final surface profile of a machined part $\mathrm{P}(x, y, z)$ is a deterministic combination of n craters $\mathrm{P}_i\left(x_i^c, y_i^c, z_i^c, h_i, d_i\right)$ and is defined as

$$\mathrm{P}(x, y, z) = \sum_{i=1\ldots n} \mathrm{P}_i\left(x_i^c, y_i^c, z_i^c, h_i, d_i\right) \tag{1}$$

where x, y, z are the coordinates of the surface profile; x_i^c, y_i^c, z_i^c are the coordinates of the crater center; and n is the number of craters.

The relative location of two consecutive craters, which is called an overlap, is also a process parameter, and can be considered either as a 2D or 3D feature. 2D spot overlap, S^{2D}, which is the percentage of overlapped XY area between two consecutive craters, is calculated by

$$S_i^{2D} = 100\% \times (d_i - \ell_i)/d_i = (1 - \ell_i/d_i) \times 100\%, \quad i = 1\ldots n-1 \tag{2}$$

where ℓ is the distance between two consecutive craters/pulses and $\ell = v/f$. 3D spot overlap, S^{3D}, which is the percentage of overlapped volume between two consecutive craters, is

$$S_i^{3D} = 100\% \times V(\mathrm{P}_{i-1} \cap \mathrm{P}_i)/V(\mathrm{P}_i), \quad i = 1\ldots n-1 \tag{3}$$

In ideal machining conditions the constant process parameters (E, f, v) corresponds to a deterministic concept of the laser precision machining when the desired (ideal) geometry of the machined part is a geometrical combination of paraboloids with constant geometry parameters (d, h). The total volume of material removed depends on the selection of the frequency of laser pulses and the travel speed for a

given focal spot diameter, which is determined by the pulse energy, beam mode, and energy distribution.

Experimental results [31-34] indicate that majority of process parameters of laser machining are not constant and also are non-deterministic. They are stochastic (random) with certain statistical signatures. Random variations within the process parameters change the geometry of each paraboloid and concomitantly change the final geometry of the machined part. The laser itself is a fairly stable dynamic system where variations of the pulse energy lie usually within 5%. Therefore, our investigations are mainly focused on the relationship between informational properties of surface acoustic waves and machining characteristics such as pulse energy and crater geometry, in order to develop more effective modelling and control strategies for the laser precision machining process.

3. EXPERIMENTAL SETUP AND PROCEDURE

The basic principle of acoustic emission is that a short laser pulse irradiates the workpiece surface. The interaction of the focused beam with material includes rapid melting, ablation and evaporation of material, and the formation of vapour-plasma plume and leads to the creation of a shock wave in the air, in the material and on the surface [2, 13-22]. The sound waves within a frequency range of up to 20 KHz are detectable by a wideband microphone. The acoustic waves, such as transverse, longitudinal and surface (Rayleigh wave), have much a broader frequency range, which is up to 1 MHz, and can be measured by an acoustic emission transducer.

Figure 2 shows the experimental setup used for the measurements of surface acoustic waves. Thin copper foil with a thickness of 70 μm was used in this study for machining. The foil was mounted on a specially built vacuum fixture. The laser-machining experiments were carried out using a Q-switched diode pumped solid state Nd:YAG laser (a HPO-1000 laser from Continuum Inc.). The laser has a pulsewidth of 9.8 ns with a wavelength of 532 nm and a shot-to-shot stability of 5.0% for TEM00 mode. The fixture was placed on a multi-axis positioning system. The worktable consisted of a granite base fitted with precision translation stages (with air bearings) for X and Y movements. The motion system had a positioning accuracy in the order of 0.5 μm in the X and Y axes. Both the laser and the motion systems were controlled using an in-house developed software, which allowed the operator to set up the process parameters and required toolpath.

The data, related to surface acoustic waves, was acquired using a high-fidelity acoustic emission (AE) transducer SE1000-HI made by Dunegan Engineering Consultants Inc., and was recorded by a digitizing oscilloscope Tektronix TDS 724C with a maximum sampling frequency of 500 MHz. The sensor has a maximum frequency of 500 KHz and a dynamic range of 74 dB. The sensor was mounted on a machining surface 30mm away from the processing area. The continuous signal from the sensor was triggered with the laser pulse and discretized in time and amplitude, producing time series. Each time series was

collected for a duration of 1 ms, giving 5000 points with a sampling interval of 0.2 μs (sampling frequency of 5 MHz), which is greater than the highest frequency that can be reliably registered with the sensor and analysed afterward. The recorded data was statistically analysed using MATLAB™ (The MathWorks Inc.) signal processing routines.

All the measurements of the pulse energy were carried out using a Gentec laser power meter TMP-300. An Olympus optical microscope (model PMG 3) and a WYKO surface profilometer were utilized to measure the geometry and surface topology of the machined craters. Experiments were carried out by applying a single laser pulse to form a crater, and measuring the surface acoustic waves simultaneously. The part was then moved to a new position for the subsequent pulse and measurement. The distance between craters was selected at 100 μm to avoid overlapping of the heat-affected zones. The craters were machined in a matrix order, where each row corresponds to a specified pulse energy and has fifty-one craters. Eight rows were machined in accordance with the following pulse energies (μJ): 604; 525; 432; 341; 262; 192; 134; 86. Fifty one machined craters were chosen experimentally to obtain consistent and sufficient statistical data about the crater dimensional parameters.

As the laser machining process involves a large number of parameters, such as pulse frequency, pulse duration, focal distance, focal spot size, travel speed, workpiece material properties, *etc*. All these parameters mutually affect the final geometric quality of the machined part and mutually generate informational signals from the laser-material interaction zone, such as light, thermo, sonic and acoustic emissions. Therefore, during actual laser machining it is almost impossible to extract specific informational properties from the measuring signal which are related to specific machining parameters without preliminary laboratory experiments. For example, in the case of a study of acoustic emission during laser welding [35], the output signal is a combination of several overlapped acoustic waves. This factor significantly reduces the frequency bandwidth of the measured signal because of the integration and mixing of a number of high-frequency signals. Specific properties of the measured signal with respect to a specific machining parameter could be obtained from preliminary laboratory experiments and that is a foundation for on-line monitoring and control of the laser-machining process. The laser pulse energy is one of the most effective and at the same time easily controllable process parameters of laser precision machining, and also significantly contributes to the accuracy, precision and the surface finish of laser-machined parts [1-4]. Therefore, experiments, reported in this paper, are focused on informational properties of surface acoustic waves generated by the interaction of a single laser pulse and the workpiece material, in order to explore the correlation with pulse energy for future applications in the area of on-line monitoring and control of laser precision machining.

4. ANALYSIS, RESULTS AND DISCUSSION

4.1. SPECTRAL ANALYSIS OF AE SIGNAL CAUSED BY A SINGLE LASER PULSE

Spectral analysis [36] was applied to obtain characteristic information of surface acoustic waves during single pulse – material interaction in the frequency domain by calculating a power spectrum. The typical acoustic wave, shown in Figure 2 and used for this analysis, was measured for a pulse energy of 525 μJ specially to obtain and compare signal properties before and after the laser pulse was applied. As can be seen, the laser pulse, which has a pulsewidth of 9.8 ns, generates an acoustic emission signal, which characterizes a surface acoustic wave, with a signal duration of 0.5 ms. This fact confirms that certain physical-chemical processes have taken place after application of the laser pulse and the corresponding laser-material interaction. Therefore, these processes are primary sources of surface acoustic waves.

In order to quantify the change of the statistical and spectral signatures during the signal duration, the signal is divided into eight consecutive time intervals. Each interval has a duration of 0.1024 ms (sampling time) giving 512 points with a sampling interval of 0.2 μs (sampling frequency of 5 MHz). Statistical signatures of the AE signal are studied by evaluating the variance of each of the above-mentioned time interval. Figure 3 illustrates a change of variance for each time interval. As can be seen in Figures 2 and 3, each laser pulse generates a non-stationary random AE signal with time-varying variance. Naturally, the behavior of variance in the time domain corresponds to the physical processes within the laser-material interaction zone and evidently has two phases – evolutional and revolutional. The evolutional phase starts with laser pulse irradiation and corresponds to the period when the material absorbs energy from the laser pulse. During this phase the variance is increasing in time. The boundary between evolution and revolution phases is maximum variance. The revolutional phase corresponds to the period when the material releases energy, material evaporates and melts, and the corresponding surface acoustic waves are generated. The decrease in variance represents this phase. The moment when the variance reaches the initial value (before laser pulse was applied) shows a reliable indication of the signal end, and this fact is used further to estimate the duration of the AE signal.

Figure 4 shows the change of the AE signal in the time and frequency domains represented by time realization and corresponding power spectrum for each time interval of signal. In order to evaluate the spectral signatures only, before calculating a power spectrum, the original time interval, $\mathbf{x} = [x_i]$, $i = 1...512$, is tabulated in terms of the normalized (standardized) variable [36]

$$z_i = \frac{x_i - \mu}{\sigma} \tag{4}$$

where μ and σ are the mean value and standard deviation of $\mathbf{x}$ respectively. This mathematical procedure produces dimensionless time series with a zero mean value, $mean(\mathbf{z}) = 0$, and a unit variance, $var(\mathbf{z}) = 1$. As can be seen in Figure 4, initially (time interval 0 ... 0.1024 ms, before a laser pulse is applied), the AE signal is random noise because of a nearly even distribution of its power

spectrum with a maximum amplitude level of 0.3×10^{-5} (dimensionless) within a frequency range of up to 500 KHz. During the next time interval (0.1026 ... 0.2048 ms, where the laser pulse has been applied), the AE signal immediately and significantly changes its spectral signature, and the power spectrum then has a dominant frequency of 375 KHz. Contrarily, the subsequent time interval (0.2050 ... 0.3074 ms) changes its spectral signature again and then the power spectrum has a dominant frequency of 98 KHz. At the beginning of the next time interval (0.3076 ... 0.4096 ms), the AE signal changes its statistical signature again and it has the two above-mentioned dominant frequencies simultaneously. During the next three consecutive time intervals (0.4098 ... 0.7168 ms), the changes in the spectral signatures are located mainly around these two dominant frequencies and are represented by variations of amplitudes. It is also necessary to note that there is one more indication that the revolutional phase is finished or almost finished. Starting at the time interval 0.4098 ... 0.5120 ms, a low-frequency diapason of up to 30 KHz begins to grow. That is the moment when sound waves, represented by the sonic emission, have begun to be generated during the laser-material interactions. This fact indicates that the sonic emission is a secondary source of information and has no advantages over the surface acoustic waves to characterize the laser material interactions. Finally, at the last time interval (0.7170 ... 0.8192 ms), the low-frequency diapason of up to 30 KHz has been formed, and there are no indications of previously observed dominant frequencies of 98 KHz and 375 KHz. All the above-mentioned details characterize the non-stationary time-varying random signature of acoustic emission signals and acoustic surface waves generated by the laser-material interactions.

4.2. EFFECT OF VARIATION IN LASER PULSE ENERGY

Figure 5 shows the change of the AE signal in the time domain with respect to the laser pulse energy within a range of 86 to 604 μJ. Observations of the AE signal reveal that laser pulses with certain energy produce an AE signal with definite duration and unique amplitude and spectral properties. In order to estimate the effect of variation in laser pulse energy on the informational properties of the AE signal, several statistical techniques were applied.

A moving variance was calculated for each of the consecutive 512 points along the time realization of the AE signal in order to estimate the signal duration. Figure 6 shows the moving variance of the AE signal for different pulse energies (86, 262, 432, 604 μJ). Figure 6 also shows that when varying the pulse energy, the signal duration is not changed because all significant changes in the variance are located within a time duration of 0.5 ms. This observation is important because it proves that the laser-material interaction process has a constant duration due to a constant laser pulsewidth of 9.8 ns. It also proves that the source for the AE signal steams from physical processes, such as melting, ablation and evaporation, within the processing zone. When changing the laser pulse energy, the laser pulsewidth is not changed; therefore, the nature and time of laser-material interactions remains permanent. In contrast, the pulse energy significantly changes the variance of the AE signal as shown in Figure 7. For this reason, the variance of the AE signal for a duration of 0.5 ms was selected as the first informational

parameter, I_1, in order to analyse the properties of the surface acoustic waves as a function $I_1(E)$. According to the theory of information [37], the variance is one of the most valuable informational parameters which characterizes the average energy of a signal. Therefore, by measuring the variance of the AE signal, the laser pulse energy can be estimated. The approximated linear relationship between the energies of the AE signal and the laser pulse with value of $R^2 = 0.9304$ (see Fig. 7) can be explained based on principles of fundamental physics when energy has been released as much as it has been delivered. But it is necessary to remember that the surface acoustic waves are only one effect within a variety of emissions generated by the laser-material interaction. On the other hand, it is important to stress the fact that the random variations of $I_1(E)$ overlap each other when the pulse energy is more than 341 μJ (see Fig. 7). This is a very strong indication that single informational parameter, such as $I_1(E)$, cannot provide sufficient and reliable information about laser-material interactions; therefore, there is a need for a multi-variable approach when a set of informational parameters is proposed and analyzed.

It is important to study spectral properties of the AE signal because they are rich in information and can easily be measured and analysed. Figure 8 shows the change of the power spectrum of the AE signal in the frequency domain with respect to the pulse energy within a range of 86...604 μJ. Observations of the power spectrums of the AE signal reveal that each power spectrum has two dominant frequencies of 98 KHz and 375 KHz, which support the analysis in Section 4.1. The amplitudes of these frequencies are mutually related to the variation in the laser pulse energy. Also, the signals within frequency diapasons of 50-200 KHz and 250-500 KHz are sensitive to the pulse energy variation. The variances of the AE signal within the two above-mentioned diapasons represent the distribution of frequency components within the power spectrum, and therefore were selected as the second and third informational parameters, I_2 and I_3, which can be calculated as

$$I_2 = \int_{50\,KHz}^{200\,KHz} S_{xx}(f)\,df\,, \quad I_3 = \int_{250\,KHz}^{500\,KHz} S_{xx}(f)\,df \tag{5}$$

where $S_{xx}(f)$ is the power spectrum of the AE signal, and f is the frequency, Hz. There is a significant difference in the relationships for $I_2(E)$ and $I_3(E)$ (see Fig. 7). The change of variance within a 50-200 KHz range with respect to the pulse energy is fairly linear with the value of $R^2 = 0.9933$. Contrarily, the variance within a 250-500 KHz range reaches a maximum at a pulse energy of 432 μJ and falls slightly afterward. This is the reason $I_3(E)$ cannot be linearly approximated correctly. Variances I_2 and I_3 are components of the variance of the AE signal; therefore, $I_1(E)$ inherits the relationships $I_2(E)$ and $I_3(E)$.

In order to statistically analyze the informational properties of informational parameters I_1, I_2 and I_3,

classic pattern recognition analysis [38] was applied. In general terms, pattern recognition analysis is based on the linear discriminant theory and makes it possible to separate data within n-dimensional informational space into clusters with specific and unique properties. Decisions for the separation obey strict mathematical rules called linear decision functions, which were calculated using Bayesian classifiers (Bayes decision functions), and do not involve human concern and preference. Each informational parameter (I_1, I_2, I_3) cannot be used individually for proper estimation and prediction of the laser pulse energy because the experimental data is overlapped (see Fig. 7). Therefore, in order to choose the best combinations of informational parameters (from the point of view of statistics), a multi-variable approach is selected, and four different informational spaces, $\{I_1, I_2, I_3\}$, $\{I_1, I_2\}$, $\{I_1, I_3\}$, $\{I_2, I_3\}$, are analysed and compared. The ISODATA algorithm [38] was used for automatic data separation with respect to the set of the pulse energies $\mathbf{E} = E_{i=1\ldots8} = \{86, 134, 192, 262, 341, 432, 252, 604\}(\mu J)$. The coefficients of Bayes decision functions were calculated as follows:

For $\{I_1, I_2, I_3\}$:
$$
\begin{aligned}
d_1(I_1, I_2, I_3) &= -532.198 * I_1(E) - 102.101 * I_2(E) - 343.533 * I_3(E) + 473.009 \\
d_2(I_1, I_2, I_3) &= -1711.026 * I_1(E) - 550.658 * I_2(E) - 911.030 * I_3(E) + 4557.909 \\
d_3(I_1, I_2, I_3) &= -844.349 * I_1(E) - 193.803 * I_2(E) - 548.480 * I_3(E) + 1198.502 \\
d_4(I_1, I_2, I_3) &= -2059.163 * I_1(E) - 820.743 * I_2(E) - 914.305 * I_3(E) + 6377.869 \\
d_5(I_1, I_2, I_3) &= -1358.200 * I_1(E) - 354.242 * I_2(E) - 865.405 * I_3(E) + 3084.529 \\
d_6(I_1, I_2, I_3) &= -1917.674 * I_1(E) - 692.811 * I_2(E) - 986.918 * I_3(E) + 5734.990 \\
d_7(I_1, I_2, I_3) &= -1053.266 * I_1(E) - 240.050 * I_2(E) - 678.036 * I_3(E) + 1851.917 \\
d_8(I_1, I_2, I_3) &= -2088.142 * I_1(E) - 964.757 * I_2(E) - 884.737 * I_3(E) + 6696.105
\end{aligned}
$$
(6)

For $\{I_1, I_2\}$:
$$
\begin{aligned}
d_1(I_1, I_2) &= -538.116 * I_1(E) - 104.120 * I_2(E) + 335.883 \\
d_2(I_1, I_2) &= -1723.750 * I_1(E) - 554.755 * I_2(E) + 3582.198 \\
d_3(I_1, I_2) &= -853.576 * I_1(E) - 197.204 * I_2(E) + 848.585 \\
d_4(I_1, I_2) &= -2069.090 * I_1(E) - 821.700 * I_2(E) + 5378.750 \\
d_5(I_1, I_2) &= -1372.314 * I_1(E) - 359.604 * I_2(E) + 2212.058 \\
d_6(I_1, I_2) &= -1930.542 * I_1(E) - 697.137 * I_2(E) + 4585.972 \\
d_7(I_1, I_2) &= -1064.642 * I_1(E) - 244.178 * I_2(E) + 1317.070 \\
d_8(I_1, I_2) &= -2095.345 * I_1(E) - 965.757 * I_2(E) + 5749.202
\end{aligned}
$$
(7)

For $\{I_1, I_3\}$: $\quad d_1(I_1, I_3) = -532.444 * I_1(E) - 453.444 * I_3(E) + 509.542$

$\qquad\qquad\quad d_2(I_1, I_3) = -1697.760 * I_1(E) - 1212.363 * I_3(E) + 4580.434$

$\qquad\qquad\quad d_3(I_1, I_3) = -1353.406 * I_1(E) - 1144.547 * I_3(E) + 3252.784$

$\qquad\qquad\quad d_4(I_1, I_3) = -842.949 * I_1(E) - 724.534 * I_3(E) + 1279.547$

$\qquad\qquad\quad d_5(I_1, I_3) = -1051.573 * I_1(E) - 895.811 * I_3(E) + 1975.883 \qquad (8)$

$\qquad\qquad\quad d_6(I_1, I_3) = -1900.165 * I_1(E) - 1314.566 * I_3(E) + 5633.916$

$\qquad\qquad\quad d_7(I_1, I_3) = -2046.926 * I_1(E) - 1165.929 * I_3(E) + 5949.668$

$\qquad\qquad\quad d_8(I_1, I_3) = -2043.193 * I_1(E) - 1246.380 * I_3(E) + 6109.153$

For $\{I_2, I_3\}$: $\quad d_1(I_2, I_3) = -52.804 * I_2(E) - 357.955 * I_3(E) + 155.408$

$\qquad\qquad\quad d_2(I_2, I_3) = -544.196 * I_2(E) - 1013.552 * I_3(E) + 1571.757$

$\qquad\qquad\quad d_3(I_2, I_3) = -116.809 * I_2(E) - 569.542 * I_3(E) + 397.070$

$\qquad\qquad\quad d_4(I_2, I_3) = -233.330 * I_2(E) - 896.478 * I_3(E) + 1006.692$

$\qquad\qquad\quad d_5(I_2, I_3) = -820.283 * I_2(E) - 898.537 * I_3(E) + 1751.814 \qquad (9)$

$\qquad\qquad\quad d_6(I_2, I_3) = -412.195 * I_2(E) - 940.402 * I_3(E) + 1249.489$

$\qquad\qquad\quad d_7(I_2, I_3) = -673.021 * I_2(E) - 940.822 * I_3(E) + 1590.268$

$\qquad\qquad\quad d_8(I_2, I_3) = -144.306 * I_2(E) - 704.301 * I_3(E) + 604.940$

In theory [38], each Bayes decision function is a function of a minimum-distance pattern classifier. This means that $d_i(\cdot)$ estimates the distance between an analyzed point and the center of the ith cluster. Therefore the minimum, $\min(d_i(\cdot), i = 1...8)$, indicates a cluster to which the analyzed point with coordinates $\{I_{(\cdot)}(E), I_{(\cdot)}(E), I_{(\cdot)}(E)\}$ belongs.

Figure 9 shows the Bayesian classification of informational parameters I_1, I_2 and I_3 with respect to the pulse energy within three information spaces $\{I_1, I_2\}$, $\{I_1, I_3\}$, and $\{I_2, I_3\}$, which are the projections of informational space $\{I_1, I_2, I_3\}$ onto corresponding planes. Figure 9 also illustrates the ellipses of equal probability (95%) and the separating lines as the linear boundaries between clusters. These ellipses frame the area where data belongs to a certain cluster with a probability of 95% or more. Also, the intersection of ellipses represents the quality of the cluster separation. The results of the pattern recognition analysis (see Fig. 9) indicate that the combination of informational parameters $\{I_1, I_3\}$ has a lower quality of cluster separation, especially for higher pulse energies, due to significant overlapping of clusters for pulse energies of 525 μJ and 604 μJ. Therefore, this combination cannot be recommended for the purpose of monitoring laser-material interactions. More preferable sets of informational parameters are $\{I_1, I_2\}$, $\{I_2, I_3\}$ and $\{I_1, I_2, I_3\}$.

CONCLUSIONS

For the laser-material interactions investigated in this study, strong acoustic emission signals were observed, and their informational properties were analysed. From the results obtained, the following conclusions can be drawn.

1. Surface acoustic waves represented by the AE signal are a result of complex physical-chemical processes within the laser-material interaction zone and therefore have non-stationary random properties and time-varying statistical and spectral signatures.

2. AE signal contains two dominant frequencies of 98 KHz and 375 KHz, for which corresponding amplitudes are varied for the duration of the AE signal. The particular sources of these frequencies need further evaluation and validation.

3. Analysis of the informational properties of an AE signal indicates that its statistical and spectral signatures depend on the pulse energy (*e.g.* the variance of the AE signal linearly correlated with the pulse energy). Furthermore, the distribution of frequency components within the power spectrum is affected by the pulse energy as well. On the other hand, it is important to stress the fact that the pulse power does not change the duration of the AE signal.

4. The use of only one informational parameter (*e.g.* variance of AE signal) is not enough to provide sufficient, reliable information about laser-material interaction for the purpose of on-line process monitoring; therefore, there is a strong need for a multi-variable approach when a set of informational parameters is to be proposed and analyzed.

5. The results of the pattern recognition analysis grant the ability to choose the most appropriate informational parameters, which can be reliably correlated with the variations in laser pulse energy, and can be more efficient to monitor the dynamics of laser-material interactions and the process performance.

6. The presented analysis is a new method to discover informational properties of various emission signals from the laser-processing zone to characterize the effects of laser-machining parameters and materials on the overall system's performance.

7. The knowledge generated in this study lays informational basis to develop further on-line monitoring and process control systems for laser precision machining.

ACKNOWLEDGEMENTS

REFERENCES

1. W.M. Steen, 1998, Laser Material Processing, 2nd edition, Springer-Verlag, New York, NY.
2. G. Chryssolouris, 1991, Laser Machining: Theory and Practice, Springer-Verlag, New York, NY.
3. A. Gillner, 2000, Laser Micro Machining, Proceedings of the Int. Seminar on Precision Engineering

and Micro Technology, July 2000, Aachen, Germany, pp. 105 – 112.

4. T. Masuzawa, 2000, Sate of the Art of Micromachining, Annals of the CIRP, Vol. 49/2/2000, pp. 473 – 488.

5. L. Li, 2000, The Advances and Characteristics of High-Power Diode Laser Material Processing, Optics and Lasers in Engineering, Vol. 34, pp. 231 – 253.

6. M. Weck, H.-G. Mayrose, J. Schon, 1992, Task-Oriented Design and Improvements of Laser Machine Tools, In: The Industrial laser handbook, Springer-Verlag, New York, pp. 74 – 93.

7. P. Di Pietro and Y.L. Yao, 1998, Improving Laser Cutting Quality for Two-Dimensional Contoured Paths, ASME J. of Manufacturing Science and Engineering, Vol. 120, pp. 590 – 599.

8. Q. Xie, S. Li, H. Wu, Q. Yin, 1999, The Vector Spot Compensation Applied in CNC System for Laser Cutting Machine, Proceedings of SPIE, Vol. 3862, pp. 337 – 341.

9. V.P. Veiko, A.G. Yakovlev, B.P. Timofeev, S.A. Tretyakov, 1999, Optimization of Plotting Trajectory for Precision 2D and 3D Laser Cutting, Proceedings of the SPIE, vol. 3822, pp. 184 – 191.

10. P. Sheng and K. Liu, 1997, Kinematic Compensation of Repetitive Errors for Non-Circular Laser Shaping, J. of Laser Applications, Vol. 9, pp. 103 – 113.

11. J.J. Chang, B.E. Warner, E.P. Dragon, M.W. Martinez, 1998, Precision micromachining with pulsed green lasers, J. of Laser Applications, Vol. 10/6, pp. 285-291.

12. P. Di Pietro, Y.L. Yao, A. Jeromin, 2000, Quality optimization for Laser Machining Under Transient Conditions, J. of Materials Processing Technology, Vol. 97, pp. 158 – 167.

13. E.V. Bordatchev and S.K. Nikumb, 1999, Laser material-removal process as a subject of automatic control, Proc. of the ASPE 14th Annual Meeting, Monterey, California, USA, pp. 236-239.

14. P. Sheng and G. Chryssolouris, 1994, Investigation of Acoustic Sensing for Laser Machining Process. Part 1: Laser Drilling, J. of Materials Processing Technology, Vol. 43, pp. 125 – 144.

15. P. Sheng and G. Chryssolouris, 1994, Investigation of Acoustic Sensing for Laser Machining Process. Part 2: Laser Grooving and Cutting, J. of Materials Processing Technology, Vol. 43, pp. 145 – 163.

16. G. Chryssolouris, P. Sheng, F. von Alvensleben, 1991, Process Control of Laser Grooving Using Acoustic Sensing, ASME J. of Engineering for Industry, Vol. 113, pp. 268 – 275.

17. Y.F. Lu, M. Meng, M.H. Hong, T.S. Low, D.S.H. Chan, Automatic Control and Real-Time Monitoring of Laser Cleaning and Laser Ablation, Proceedings of the 1998 Materials Research Society Spring Symposium, April 13 – 16, 1998, San Francisco, CA, USA, pp. 149 – 156.

18. J.M. Lee, K.G. Watkins, W.M. Steen, P.C. Russell, G.R. Jones, 1999, Chromatic Modulation Based Acoustic Analysis Technique for In-process Monitoring of Laser Materials Processing, Journal of Laser Applications, Vol. 11/5, pp. 199 – 205.

19. J.M. Lee, K.G. Watkins, W.M. Steen, 2000, Real-Time Monitoring and Expert Control of Laser Cleaning, Proceedings of the Laser Materials Processing Conference ICALEO'2000, LIA Vol. 89, Section E, pp. 232 – 241.

20. T. Kurita, T. Ono, N. Morita, 2000, Study of Numerical Analysis of the Frequency Characteristic of Laser Processing Sound, Journal of Material Processing Technology, Vol. 101, pp. 193 – 197.

21. T. Kurita, T. Ono, N. Morita, 2000, Study of the Relationship between Laser Processing Sound and Material Removal Characteristics, Journal of Material Processing Technology, Vol. 97, pp. 168 – 173.

22. V.M. Weerasinghe, J.N. Kamalu, R.D. Hibberd, W.M. Steen, 1990, Acoustic Signal from Laser Back Reflection, Optics and Laser Technology, Vol. 22, No. 6, pp. 381 – 386.

23. I. Decker, H. Heyn, D. Martinen, H. Wohlfahrt, 1997, Process Monitoring in Laser Beam Cutting on its way to industrial application, Proceedings of the SPIE, Vol. 3097, pp. 29 – 37.

24. H. Haferkamp, M. Goede, A. von Busse, 1999, Quality monitoring and assurance for laser beam cutting using a thermographic process control, Proceedings of the SPIE, Vol. 3824, pp. 383 – 391.

25. E. Beyer and P. Abels, 1992, Process Monitoring in Laser Materials Processing, Proceedings of LAMP'92, Nagaoka, Japan, pp. 433 – 438.

26. D. Kechwmair, G. Caillibotte, F. Bataille, 1990, Real-Time Control of High-Power Laser Materials Processing. In: Industrial Laser Annual Handbook, pp. 94 – 101.

27. F.O. Olsen, H. Jorgensen, C. Bagger, 1992, Recent Investigations in Sensorics for Adaptive Control of Laser Cutting and Welding, Proceedings of LAMP'92, Nagaoka, Japan, pp. 405 – 414.

28. G. Chryssolouris, 1994, Sensors in Laser Machining, Annals of the CIRP, Vol. 43, pp. 513 – 519.

29. Y. Zhou, P. Orban, S. Nikumb, 1995, Sensors for Intelligent Machining – A Research and Application Survey, Proceedings of the IEEE Int Conference on Systems, Man and Cybernetics, Vancouver, BC, Canada, Vol. 2, pp. 1005-1010.

30. P. Di Pietro and Y. L. Yao, 1994, An Investigation into Characterizing and Optimizing Laser Cutting Quality – A Review, Int J Mach Tools Manufact, Vol. 34/2, pp. 225 – 243.

31. E.V. Bordatchev and S.K. Nikumb, 2000, Dynamic Performance of High Precision Laser Micromachining Systems, Proceedings of the 2000 NSF Design & Manufacturing Research Conference, Vancouver, BC, Canada, pp. 17-21.

32. E.V. Bordatchev and S.K. Nikumb, 2001, Improving Geometric Quality Of Laser Micromachined Parts Using High-Precision Motion System Dynamic Performance Analysis, Proceedings of the World Manufacturing Congress 2001, April 1-4, 2004, Rochester, New York, USA (submitted for publication).

33. E.V. Bordatchev and S.K. Nikumb, 2001, Geometric Quality Analysis And Process Control For Ultra-Precision Laser Micromachining, Proc. of the ASPE 16th Annual Meeting, Crystal City, Virginia, USA, pp. 281 - 284.

34. E.V. Bordatchev and S.K. Nikumb, 1999, Laser material-removal process as a subject of automatic control, Proc. of the ASPE 14th Annual Meeting, Monterey, California, USA, pp. 236-239.

35. K. Mori and I. Miyamoto, 1997, In-process Monitoring of Laser Welding by the Analysis of Ripples in the Plasma Emission, Journal of Laser Applications, Vol. 9, pp. 155-159.

36. J.S. Bendat and A.G. Piersol, 1993, Engineering Applications of Correlation and Spectral Analysis, 2nd ed., John Wiley & Sons, New York

37. S. Guiasu, 1977, Information theory with applications, New York: McGraw-Hill

38. J.T. Tou and R.C. Gonzalez, Pattern recognition principles, Addison-Wesley Pub. Co., Reading, MS, 1974.
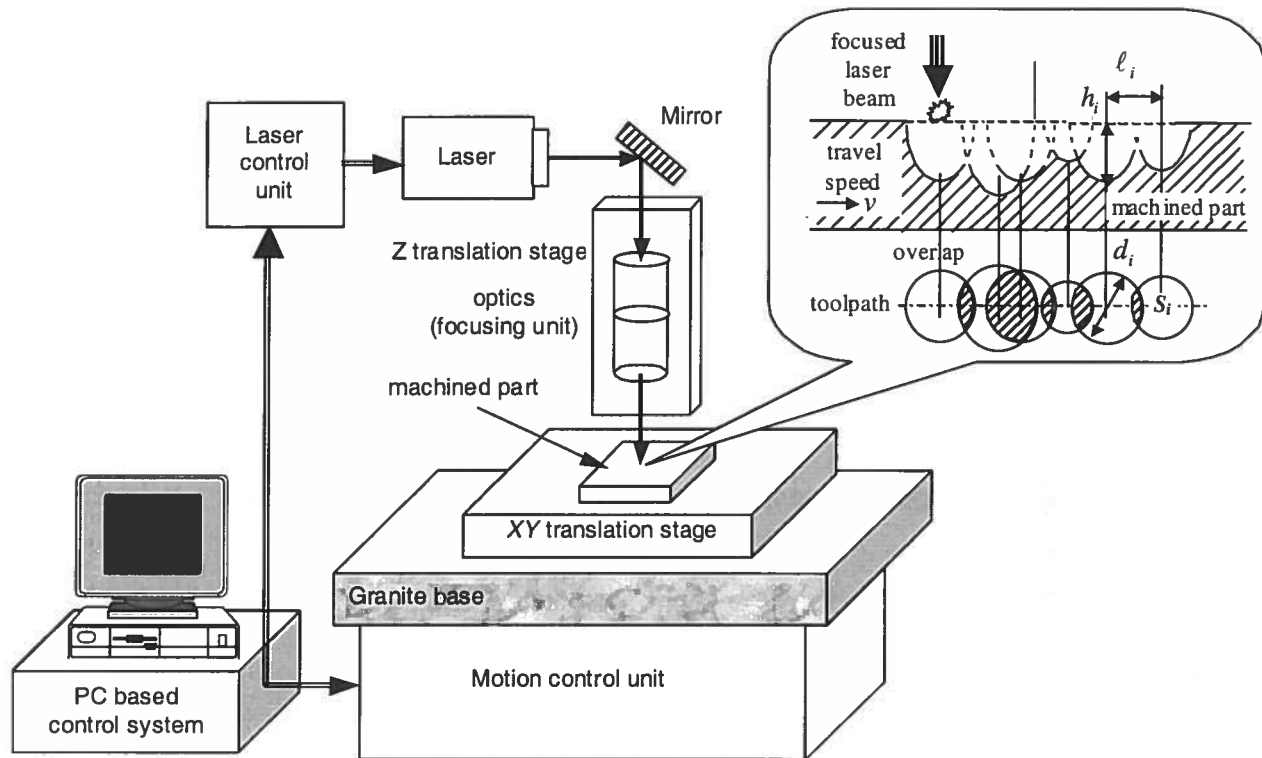
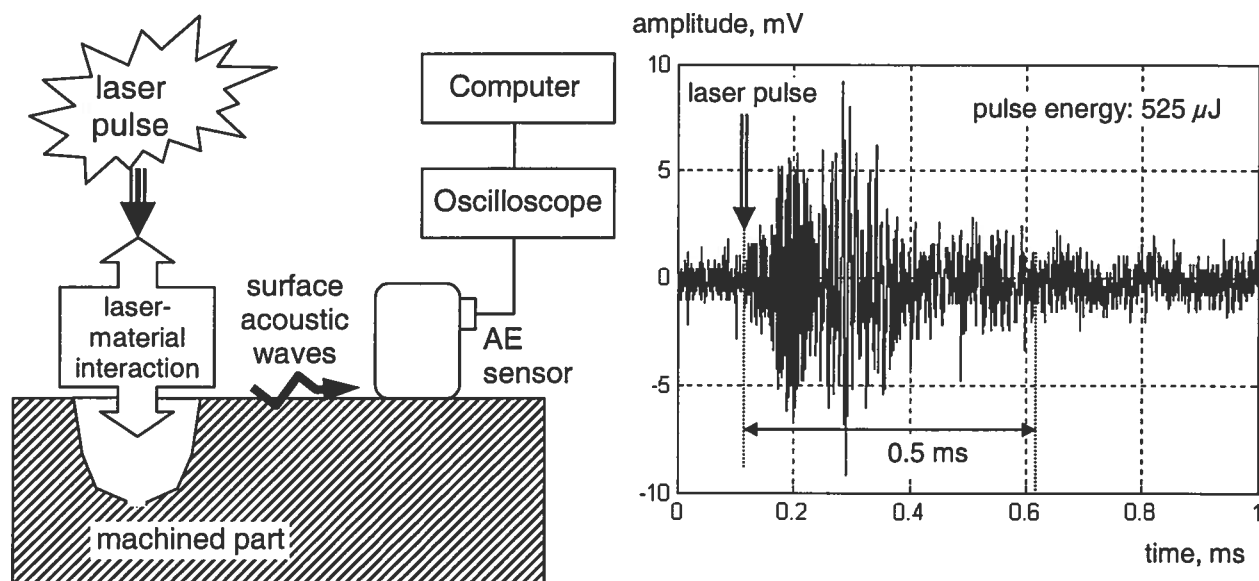Fig. 1. Schematics of the laser precision machining.
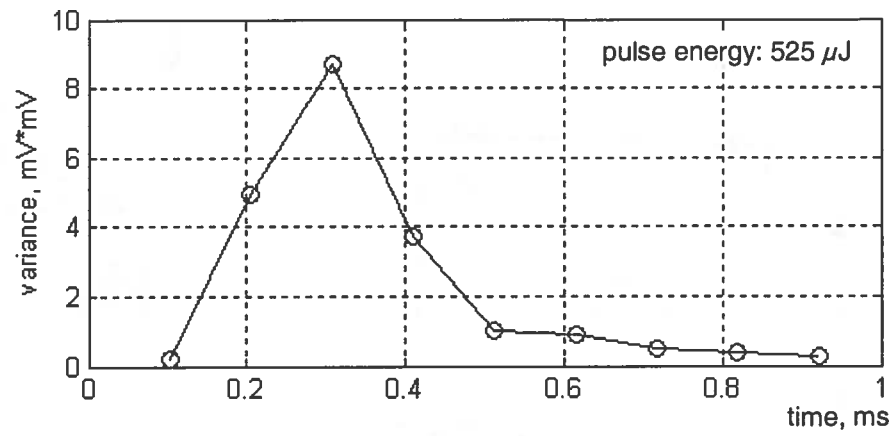

Fig. 2. Schematics of the experimental setup.

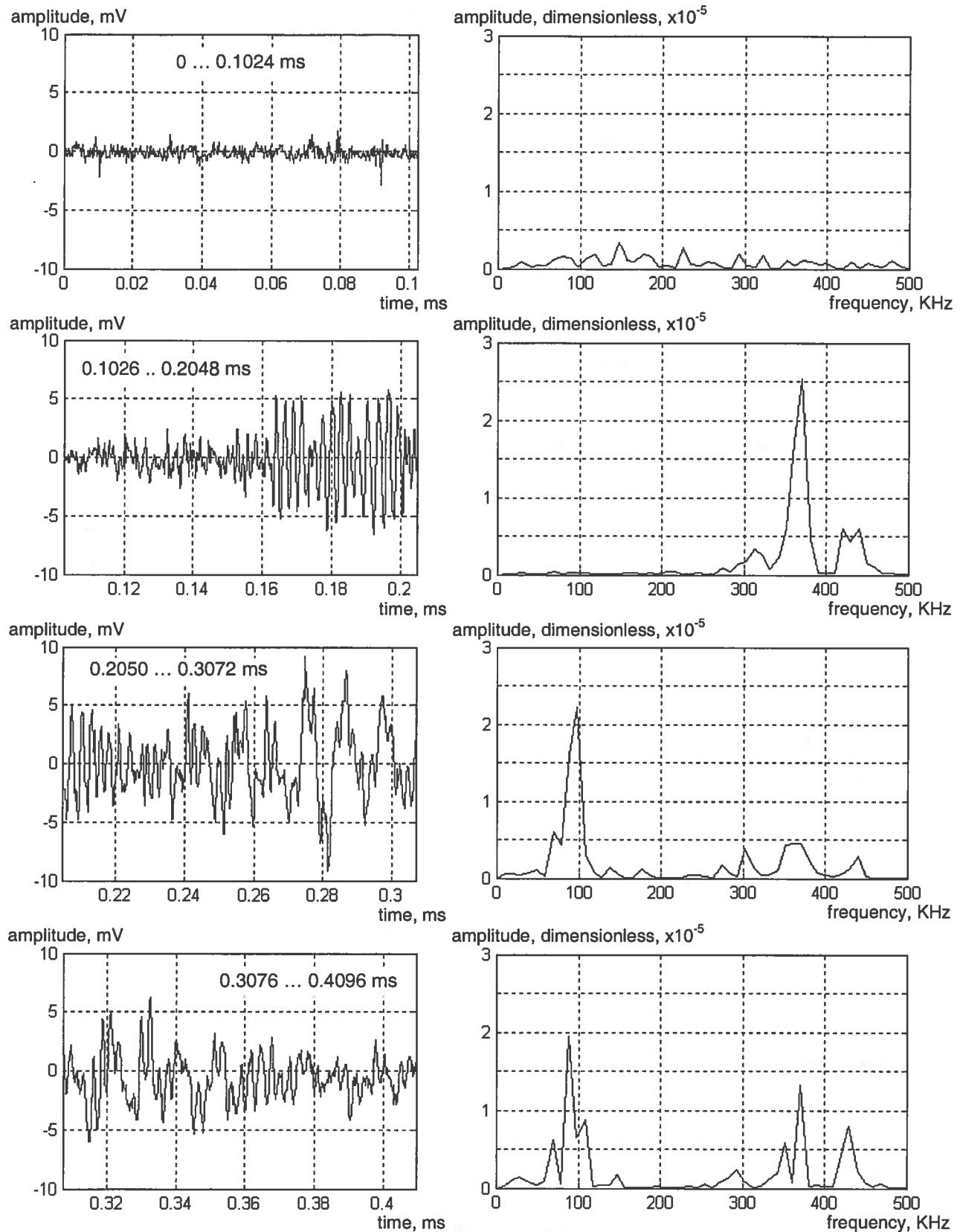Fig. 3. Change of the variance for each time fragment of the AE signal.

Fig. 4. Change of the AE signal in time (left column) and frequency (right column) domains.
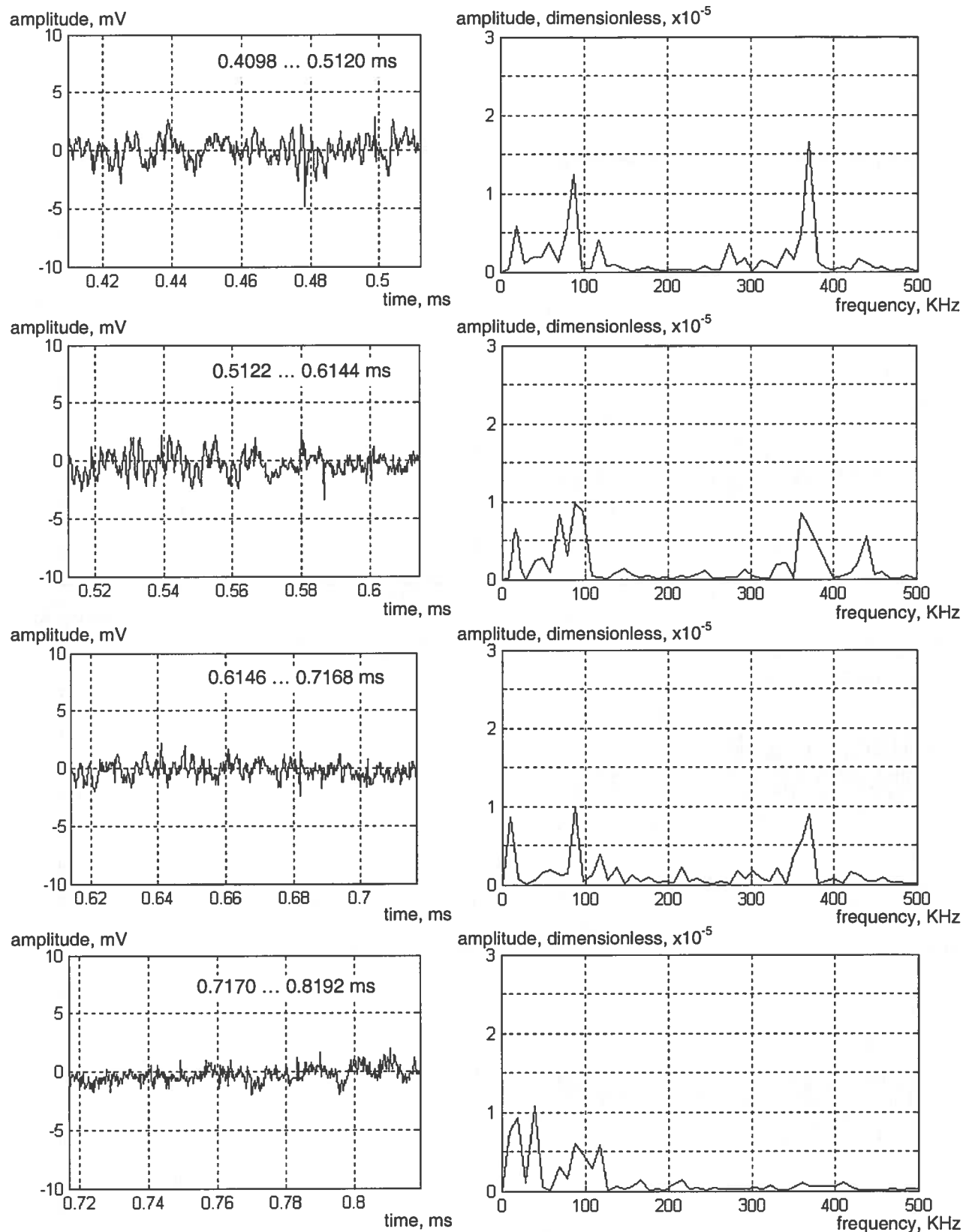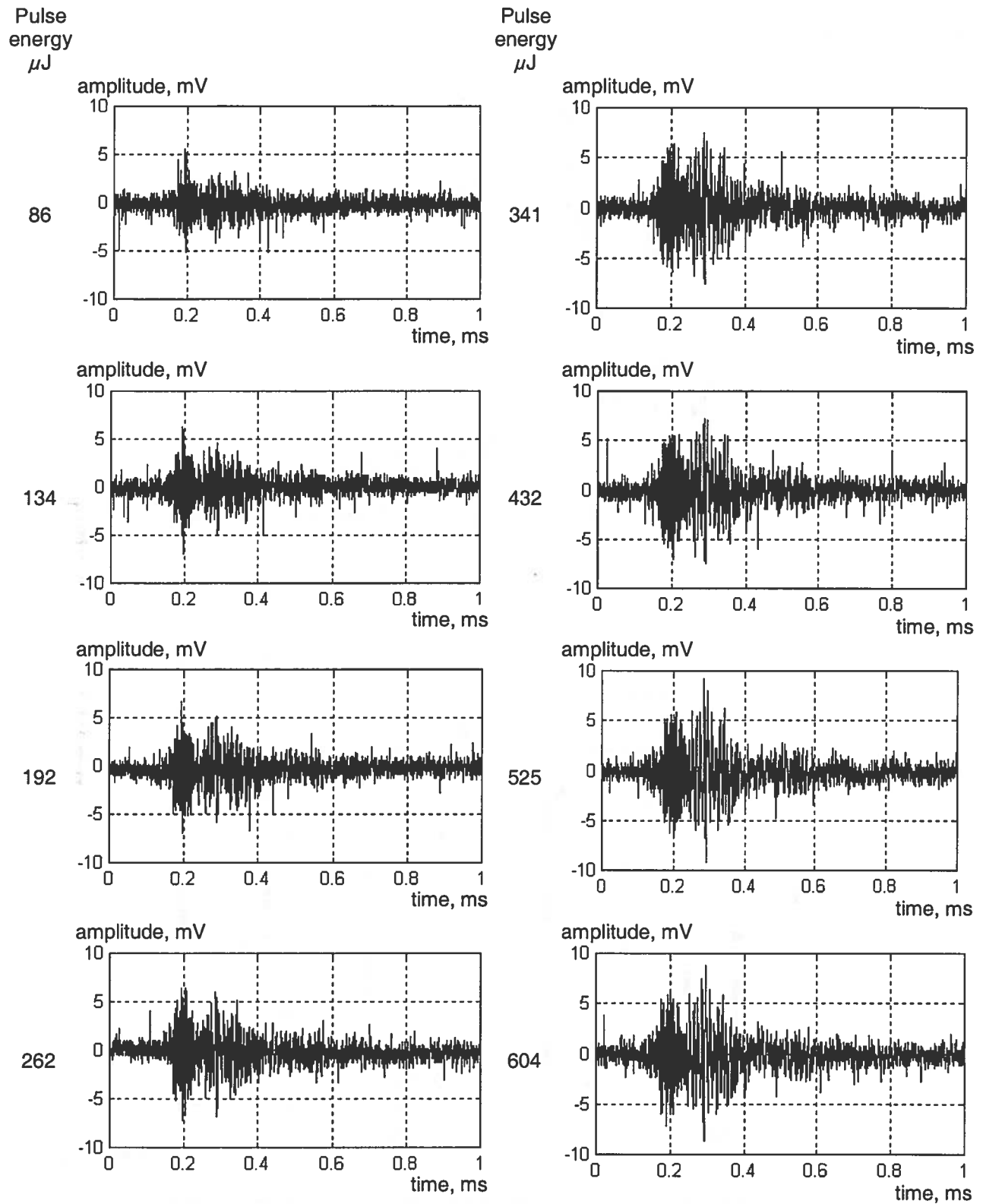(Note: Figure 4 is continued on the following page)

Fig. 4. Continued

Bordatchev & Nikumb: Informational Properties of Surface Acoustic Waves Generated by Laser-Material Interactions During Laser ...   17

12/10/2001

Fig. 5. Change of the AE signal in time domain with respect to the laser pulse energy.

Fig. 6. Moving variance of the AE signal for different pulse energies.

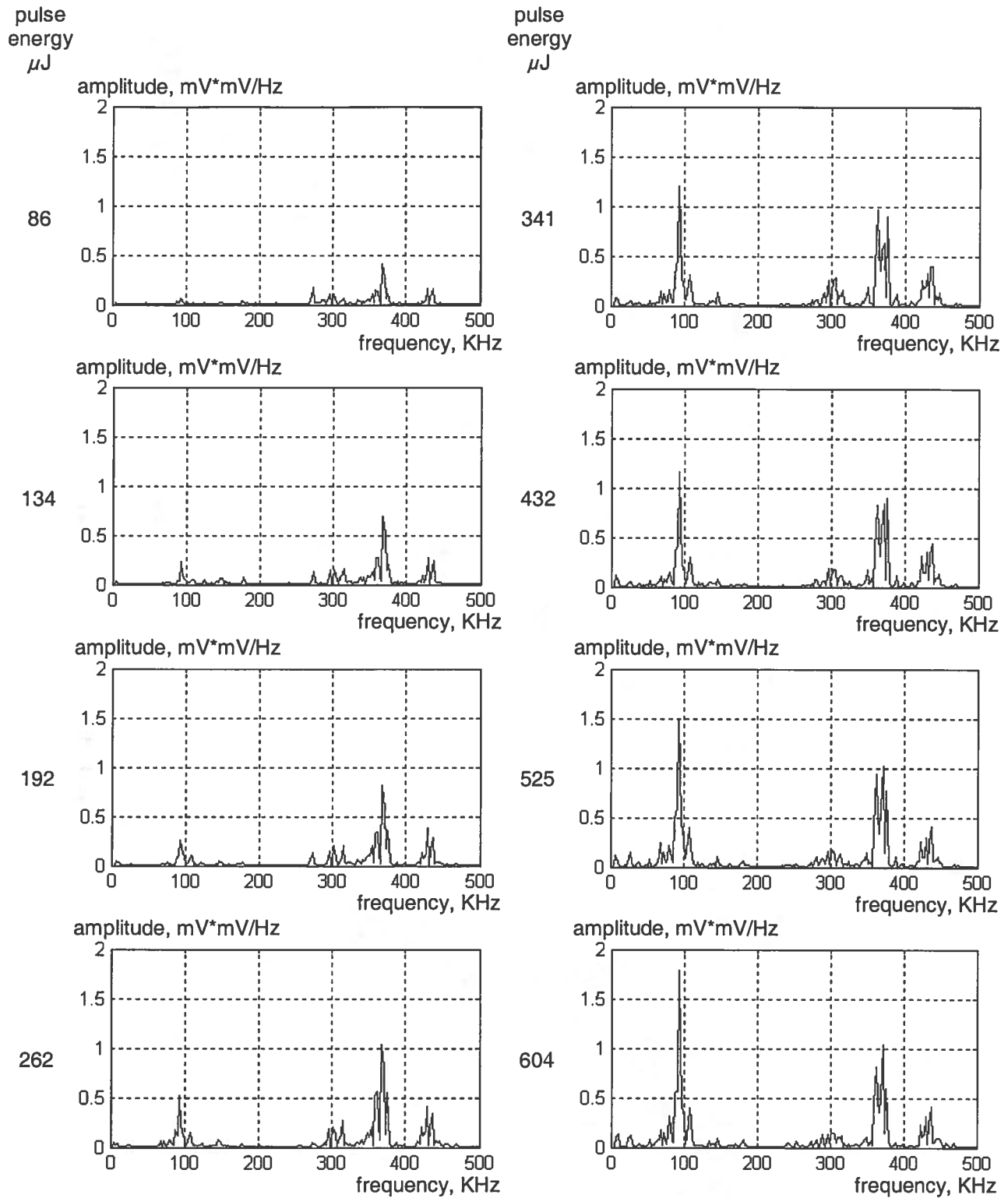Fig. 7. Change of the AE signal variances with respect to the laser pulse energy.
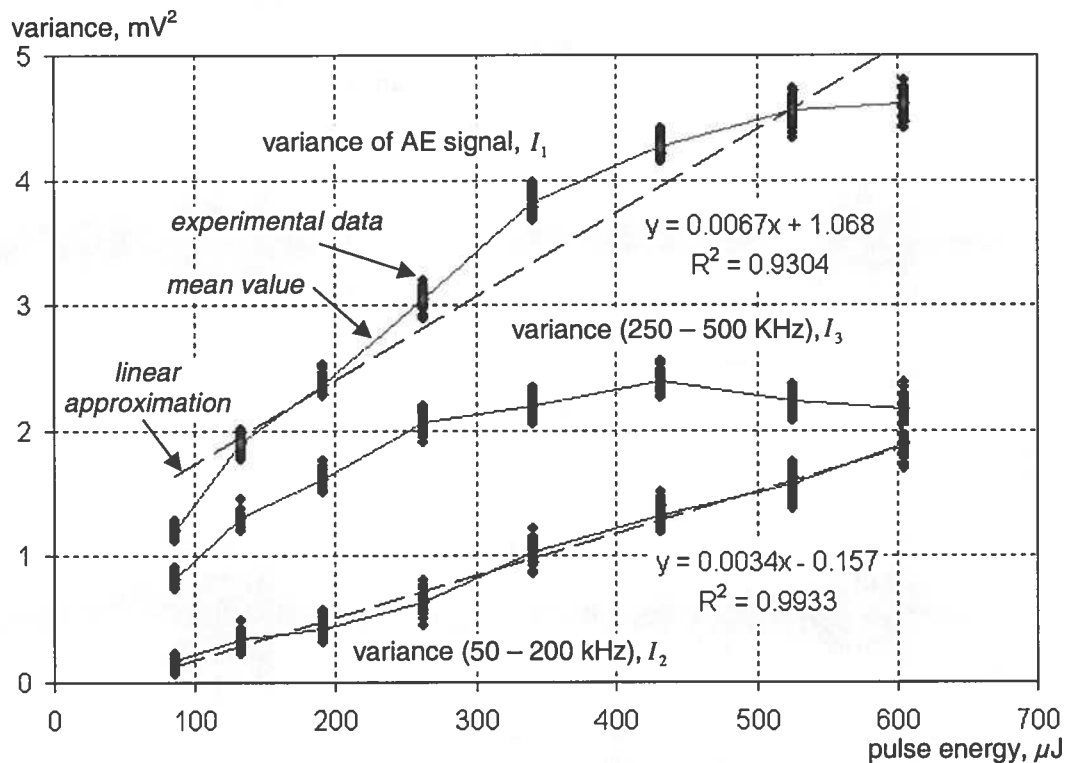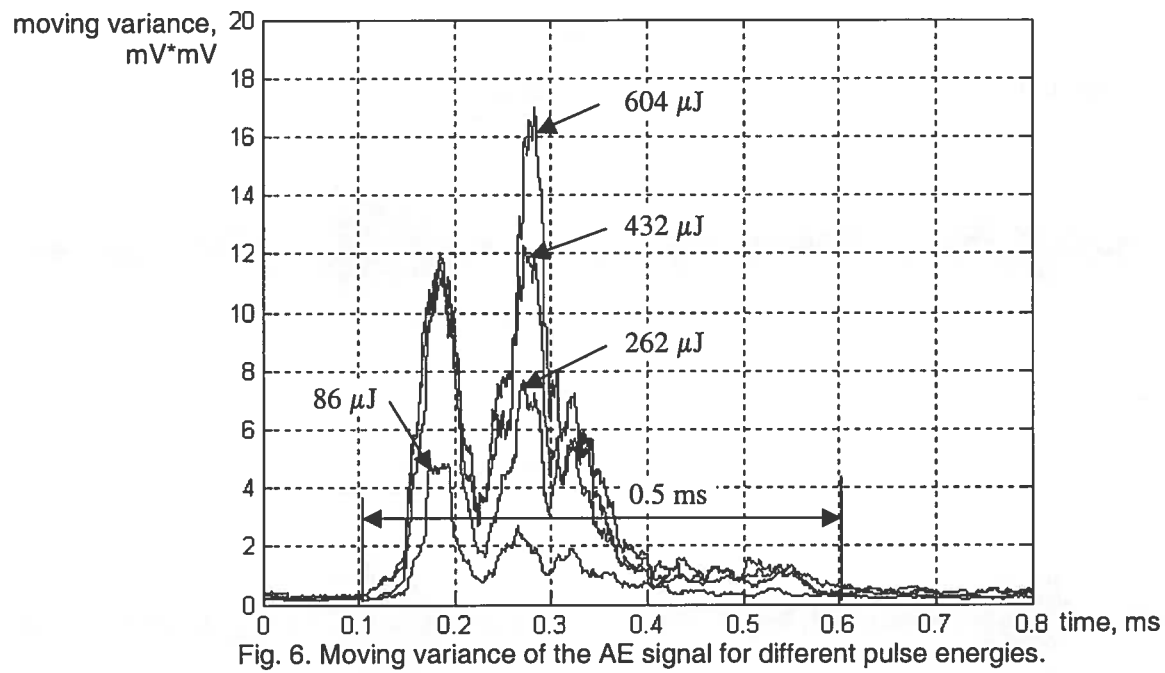
Fig. 8. Change of the power spectrum of the AE signal with respect to the laser pulse energy.
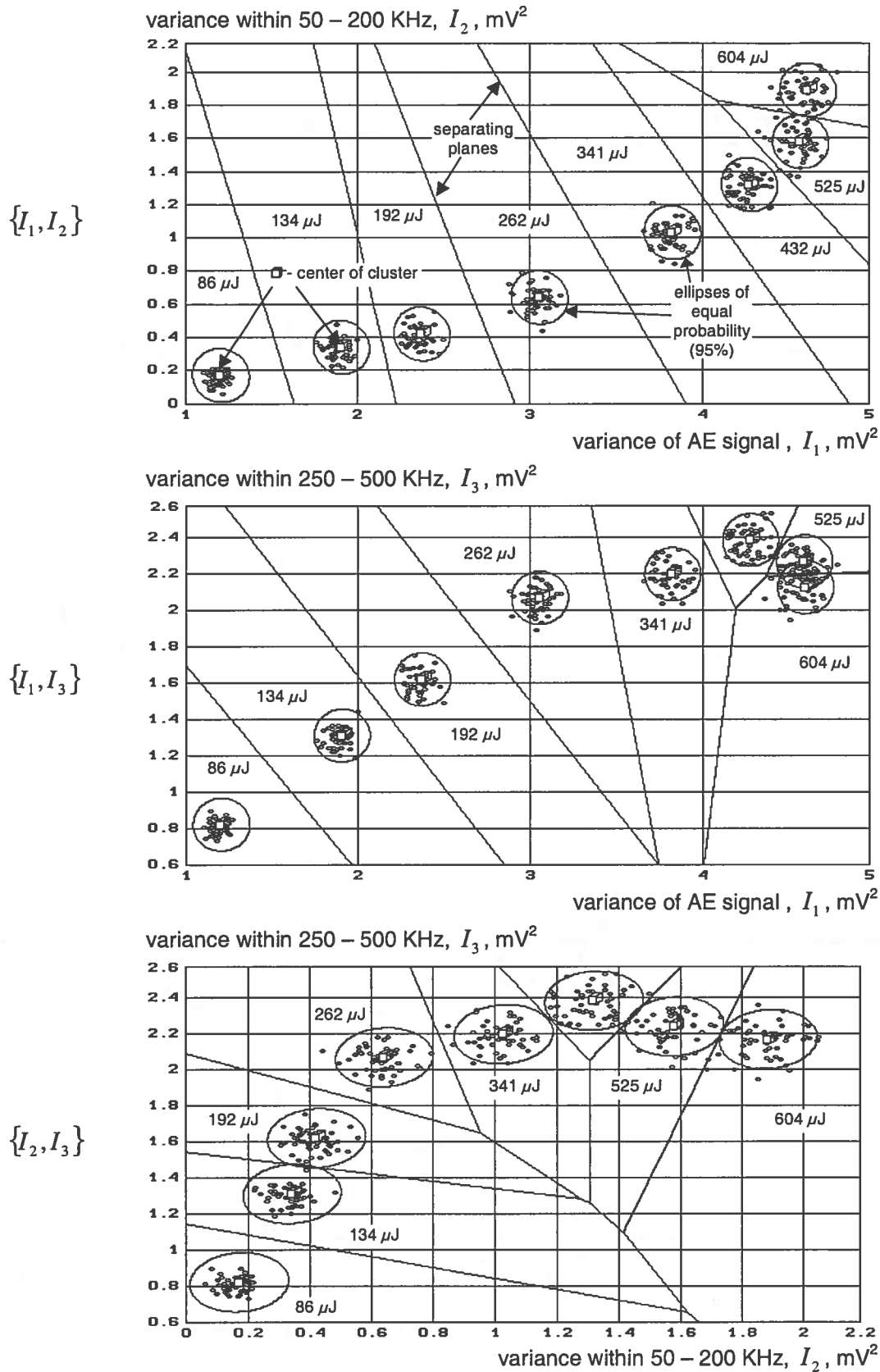
Fig. 9. Bayesian classification of informational parameters I_1, I_2 and I_3 with respect to the pulse energy.

Bordatchev & Nikumb: Informational Properties of Surface Acoustic Waves Generated by Laser-Material Interactions During Laser ...

12/10/2001

21